

ORIGINAL ARTICLE

Energy harvesting from conducted electromagnetic interference of fluorescent light for Internet of Things application

Chang-Hee Hyoung  | Jung-Hwan Hwang 

Telecommunications and Media Research Laboratory, Electronics and Telecommunications Research Institute, Daejeon, Republic of Korea

Correspondence

Jung-Hwan Hwang, Telecommunications and Media Research Laboratory, Electronics and Telecommunications Research Institute, Daejeon, Republic of Korea.

Email: jhhwang@etri.re.kr

Funding information

Korea government (MSIT), Grant/Award Number: 2021-0-00103

Abstract

A novel energy harvesting technique that uses conducted electromagnetic interference as an energy source is presented. Conducted EMI generated from fluorescent light using a switched-mode power supply was measured and modeled as an equivalent voltage source. Two types of rectifier circuits—a bridge rectifier and a voltage doubler—were used as the harvesting devices for conducted EMI source. The matching networks were designed based on the equivalent model, and the harvested power was improved. The implemented energy harvester produces a regulated power over 68.9 mW and current over 15.1 mA while a regulated voltage can be selected between 3.3 V and 5 V. The proposed system shows the highest harvesting power indoor environment and can provide enough power for the Internet of Things devices.

KEYWORDS

conducted EMI, energy harvesting, rectifiers, Schottky diodes, switched-mode power supply

1 | INTRODUCTION

The Internet of Things (IoT) technology enables various objects including sensors to connect to each other and transfer data between them without any human intervention. Examples of those objects are indoor sensors: occupancy sensors and motion sensors for controlling light systems, temperature sensors as well as humidity sensors for monitoring the environmental conditions, and smoke detectors for fire alarms. Many IoT devices are installed on the ceiling indoors. Power is supplied to those IoT devices to operate device functions and also data communication. Energy harvesting is a good power-supplying technology for IoT device applications because no power line is required to install the devices on the ceiling [1, 2].

Many studies have considered various ambient harvesting sources such as solar, thermal, and vibration ones for indoor energy harvesting. Solar energy harvesting is the most common technology because a photovoltaic (PV) cell is cost-effectively producing high energy. An indoor application of solar energy harvesting, however, has limitations in that its harvesting energy is significantly reduced [3]. To overcome this limitation, hybrid approaches have been proposed to collect energy from two or more sources indoors in such a way that selects one of them [4], adds all of them [5], or does both simultaneously [3,6]. Even multi-source harvesting, however, produces power, not more than a few mWs due to the inherent weakness of the indoor energy sources.

More power can be harvested from a fluorescent light, which is the most commonly used artificial light indoors.

Thermal energy from illuminating light or spurious electromagnetic (EM) waves radiating from a fluorescent light can be a source for energy harvesting. The harvesting from a fluorescent light has two types: portable and fixed types, respectively. The thermal energy harvesting using PV cells corresponds to the portable type [3,7–9]. Spurious EM waves are radiated from a fluorescent light, and those radiated waves are received for energy harvesting using an antenna [10]. This energy harvesting also corresponds to the portable type. In the fixed type, the same spurious EM waves are received by a fixed antenna that is installed right beneath a fluorescent light [11,12]. Another fixed type harvests power from magnetic fields that are formed around a power line, which is connected to a fluorescent light [13,14].

This paper presents a harvesting technology using a conducted signal that flows on the surface of a fluorescent lighting device. The conducted signal originates from conducted electromagnetic interference (EMI). As shown in Figure 1, the energy harvester proposed in this paper is electrically connected to the surface of the fluorescent light through the adhesive conductive electrode. When a switched-mode power supply (SMPS) inside is operational, an EMI signal is generated and coupled to the metal surface composing the fluorescent light. As shown in Figure 1, this EMI signal is received at the energy harvester and then transformed into power. The proposed harvesting technology is advantageous in that harvesting power reaches several dozens of mWs, which is much higher than harvesting power in previous fixed-type harvesters. The rest of this paper is organized as

follows. Section 2 presents measurement and analysis results on the conducted EMI signal of a fluorescent light that is used as a harvesting source in our study. Section 3 models the harvesting source based on the source measurement results, and designs circuits composing an energy harvester. Section 4 measures harvesting power using the designed harvester and then compares it with previous studies. Finally, Section 5 concludes this paper.

2 | MEASUREMENT AND ANALYSIS OF CONDUCTED EMI SIGNAL

In fluorescent light, an SMPS converts a 60-Hz alternating current (AC) into a low frequency (LF) one between 30 kHz and 100 kHz. The converted LF current starts an electronic ballast inside the fluorescent light. The frequency conversion causes radiation of EM waves out of the SMPS. An EMI filter reduces this radiation [15], but a part of the EM waves still leak out of the SMPS. The leaked EM waves are coupled with a metal body of the fluorescent light such as a lampshade, and finally, the coupled signal generates a conducted current on the surface of the metal body. This conducted current is received and processed by an energy harvester. In this way, energy harvesting is possible from the conducted EMI signal in the fluorescent light.

The energy harvesting proposed in this paper is similar to the harvesting from spurious EM waves in [11,12]. The proposed harvesting, however, requires no antenna. Instead, the energy harvester requires electrical contact with the metal body of a fluorescent device. As shown in Figure 1, the conductive adhesive electrode can be used to make electrical contact between the metal body and the energy harvester. The conducted current flows along the conductive path on the surface of the metal body without any free-space loss that is experienced by a radiating signal. As a result, more power can be harvested in comparison with the energy harvesting from spurious EM waves. No antenna requirement is also beneficial, because a large-sized antenna is required if spurious EM waves in the LF band are to be received for the energy harvesting.

Prior to designing the energy harvester, the conducted EMI signal was measured using the measurement setup shown in Figure 2. The fluorescent light was placed inside an anechoic chamber along with the spectrum analyzer and the oscilloscope. The fluorescent light had a nominal input power of 64 W. To receive the conducted EMI signal, the conductive adhesive electrode was attached to the lampshade of the fluorescent light. The electrode included a conductive area of $10 \times 10 \text{ mm}^2$, and this conductive area was electrically connected to the

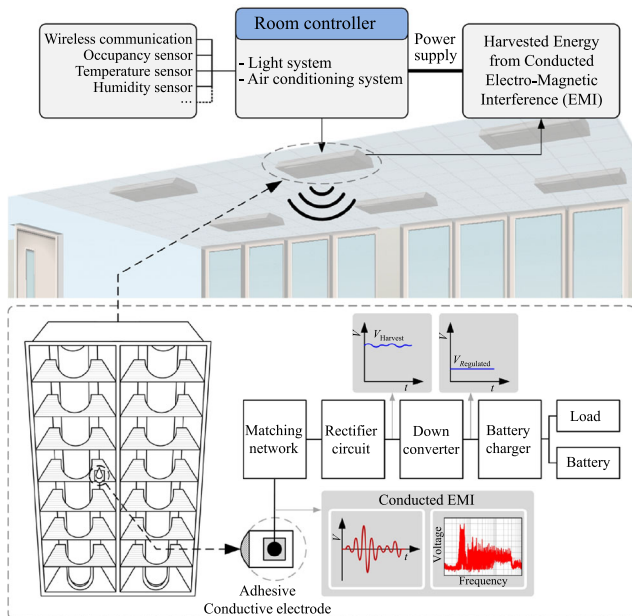


FIGURE 1 Energy harvesting from conducted EMI of fluorescent light

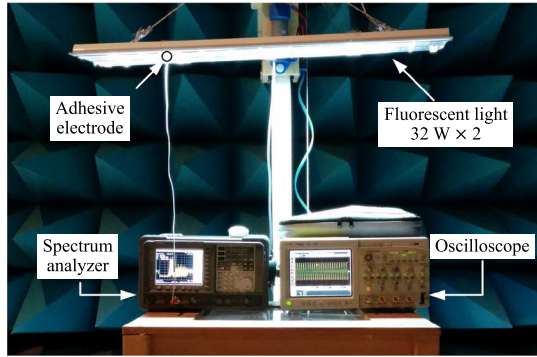


FIGURE 2 Measurement setup to measure conducted EMI signal of fluorescent light

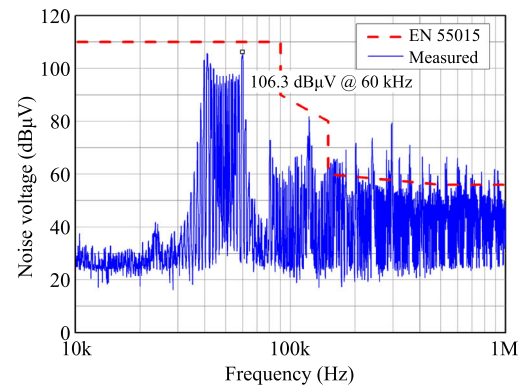
lampshade. The conducted EMI signal received at the electrode was measured using the spectrum analyzer and the oscilloscope, respectively.

Figure 3 shows the measurement results. Each subfigure shows the conducted EMI signal in the frequency and time domains, respectively, which were measured using the spectrum analyzer and the oscilloscope, respectively. As shown in Figure 3A, two peaks exist at about 40 kHz and 60 kHz, respectively. Such peak frequencies are reasonable because SMPS in fluorescent lights converts a 60-Hz AC into an LF one between 30 kHz and 100 kHz. The same EMI signal was measured using the oscilloscope in the time domain after setting the oscilloscope to have a 50- Ω input impedance as in the spectrum analyzer. As shown in Figure 3B, the conducted EMI signal is continuous and periodic. The periodic property is caused by the fact that the conducted EMI signal has the highest peak at about 60 kHz as shown in Figure 3A. As shown in Figure 3B, the conducted EMI signal has a high amplitude of about 1 V even with a low load impedance of 50 Ω .

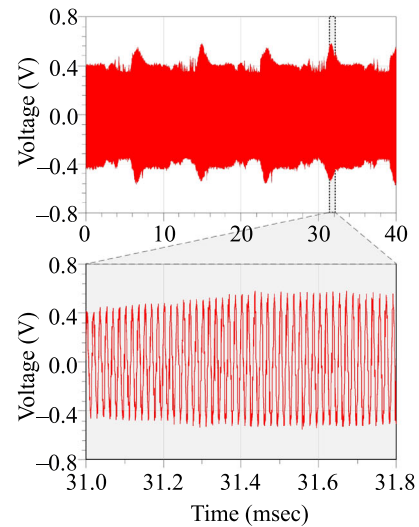
According to the EN 55015 standard in [16], all lighting equipment should meet the conducted emission limitation, which is 110 dB μ V in the quasi-peak level below 90 kHz. Figure 3A shows the conducted emission limitation of the EN 55015 standard. For the fluorescent light, the conducted EMI signal satisfies the emission limitation while having the conducted EMI signal about 1 V as shown in Figure 3B. This means that the fluorescent light can be a powerful harvesting source within the range of the conducted emission limitation.

3 | DESIGN OF ENERGY HARVESTER FOR CONDUCTED EMI SIGNAL

Figure 4A shows the structure of the energy harvester proposed in this paper. As shown in Figure 4A, the signal



(A)



(B)

FIGURE 3 Conducted EMI signal measured in (A) frequency domain and (B) time domain

of the conducted EMI source is connected to the matching network. The conducted EMI signal is received at the energy harvester through the matching network. The rectifier circuit then rectifies the conducted EMI signal. Finally, the down converter converts the rectified signal into a regulated voltage and current to supply power to the resistor load.

3.1 | Model of harvesting source

The energy harvester can be designed only after a harvesting source is modeled. Figure 4B shows the source model that is composed of the source voltage V_{CI} and the complex source impedance $R_{CI} + jX_{CI}$, respectively. The source resistance R_{CI} includes a resistance added by the conductive adhesive electrode shown in Figure 4A. The source impedance cannot be measured

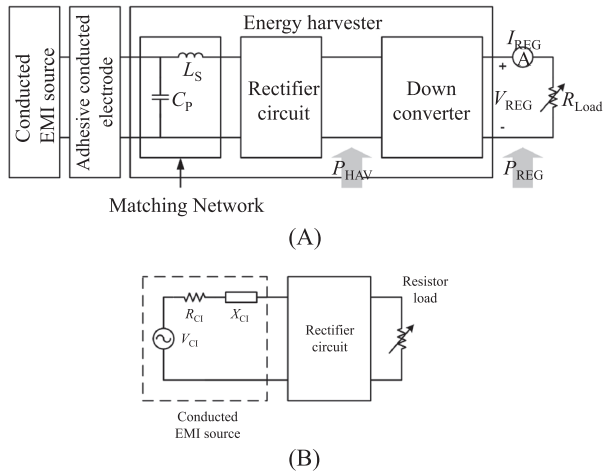


FIGURE 4 Energy harvester structure for conducted EMI signal: (A) with a matching network and a down converter and (B) source modeling structure

directly while the voltage source exists at the same time. Instead, the source impedance can be determined using an optimization process. As shown in Figure 4B, the unknown source impedance is connected to the rectifier circuit, which is described in the next section. The rectifier circuit is terminated with an arbitrary load resistance. In our study, the load resistance is set to 50 Ω . Prior to the optimization process, the power is measured at the rectifier load after connecting the rectifier circuit to the fluorescent light through the adhesive conductive electrode. The optimization process is then applied to the circuit in Figure 4B. The source impedance is optimized to make the power at the rectifier load close to the measure power. The source impedance $R_{CI} + jX_{CI}$ is determined to minimize difference between the two powers.

As shown in Figure 4A, the harvested power P_{HAV} is defined as the power at the rectifier output. The maximum P_{HAV} , $P_{HAV,MAX}$, is obtained using the determined source impedance and the maximum power transfer theory as follows.

$$P_{HAV,MAX} = \frac{|V_{CI}|^2}{4R_{CI}}. \quad (1)$$

As shown in Figure 3A, the conducted EMI signal is composed of multiple sinusoidal signals that have a different amplitude, respectively, depending on its frequency. From the superposition theory in [17], the source voltage resulting from summation of n sinusoidal signals can be approximated with an envelope that is expressed

$$V_{CI}(t) \cong \sum_{\substack{2 < i < n \\ 1 < j < i}}^n \left(\frac{2}{n-1} \right) \cdot \left\{ \sin \left[2\pi \left(\frac{f_i + f_j}{2} - t \right) t \right] \right. \\ \left. \cdot \cos \left[2\pi \left(\frac{f_i - f_j}{2} - t \right) t \right] \right\}. \quad (2)$$

From (1) and (2), the maximum harvested power can be calculated for the conducted EMI signal from a fluorescent light. Our study considers only one sinusoidal signal at 60 kHz. This is because the harvesting from a single tone signal makes it easy to design the rectifier circuit and the down converter in Figure 4A. Also, the conducted EMI signal in Figure 3A has the highest voltage at 60 kHz, so such single-tone harvesting results in a enough power to drive IoT sensors. After the optimization process, the source impedance is determined to be 1230-j 4910 while the source voltage is 20.72 V. From these values and above equations, the maximum harvesting power $P_{HAV,MAX}$ is calculated to be 87.25 mW. Each circuit in Figure 4A is designed using the source model in Figure 4B.

Figure 4B shows the source model of the conducted EMI signal. The source model is composed of the resistance R_{CI} and the reactance X_{CI} . R_{CI} includes the resistance added by the conductive adhesive electrode. The source model was developed from the measurement results shown in Figure 3. R_{CI} and X_{CI} were determined using the optimization process provided by ADS from Agilent Technologies. In the circuit simulation, the source model was connected to the rectifier circuit without the matching network. R_{CI} and X_{CI} were optimized to minimize the difference between the simulated and measured powers. The simulated power was obtained at the rectifier output with a 50- Ω load while the measured power corresponded to the power at 60 kHz in Figure 3A. The source was modeled with a single frequency of 60 kHz because the conducted EMI signal has the highest voltage at 60 kHz as shown in Figure 3A. Using the source model in Figure 4B, each circuit in Figure 4A was designed.

3.2 | Rectifier circuit

The rectifier is a key device for energy harvesting from the conducted EMI signal. A full-wave rectifier has a higher efficiency than a half-wave one. In this paper, two types of full-wave rectifiers were employed and compared: a bridge rectifier and a voltage doubler. As shown in Figure 5A, the bridge rectifier is composed of four diodes. It is widely used for rectifying an LF-band signal

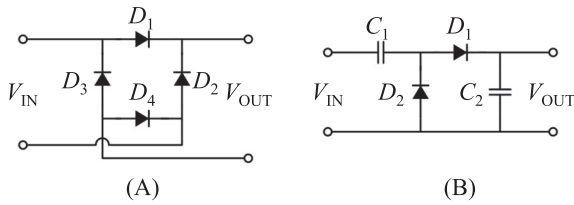


FIGURE 5 Rectifier circuits: (A) bridge rectifier and (B) voltage doubler

due to its capability to handle high power [18]. Figure 5B shows the voltage doubler that consists of a pair of series-stacked half-wave rectifiers. In comparison with the bridge rectifier, the voltage doubler is advantageous in that it uses just two diodes while rectifying a full wave. Less number of diodes results in less power consumption and consequently, higher efficiency [19, 20].

For the rectifier, a diode type should be determined considering its threshold voltage because the threshold voltage affects efficiency especially when the rectifier handles a low power. In our study, the rectifier uses Schottky diodes that have a low forward voltage drop while supporting fast switching. A Schottky diode model should be selected considering the input voltage of the rectifier circuit. When the conducted EMI source has the same output power, a high input impedance of the rectifier results in a high incident voltage to the rectifier; hence, a Schottky diode model having a high breakdown voltage should be used for the rectifier circuit. The HSMS-280x series from Avago Technologies has a high breakdown voltage of over 70 V [21]; hence, the HSMS-2808 was selected for the bridge rectifier and the HSMS-2802 for the voltage doubler, respectively.

Figure 6 shows the output voltage and power of the rectifier that were measured and simulated, respectively, using the source model in Figure 4B. In the simulation, each rectifier shown in Figure 5 terminated its output with a resistor load having increasing resistance. As shown in Figure 6A, the measured output voltage of the bridge rectifier exceeds over 60 V. If the load resistance increases, the measured output voltage of the voltage doubler reaches up to 70 V. The output voltage is measured with a load resistance of up to 150 k Ω to avoid breakdown and failure of the Schottky diode. The source model for the simulation has the minimum error over the load impedance range for maximum output power. Consequently, the output voltage error increases over a high impedance load of 100 k Ω . As the output power decreases, the inaccuracy of the source model is negligible. As shown in Figure 6B, the maximum powers are almost the same for the bridge rectifier and the voltage doubler, respectively. The maximum harvesting power

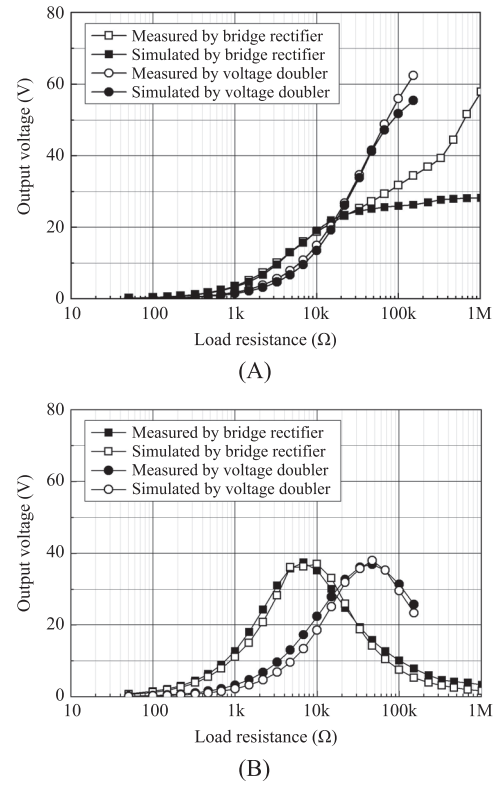


FIGURE 6 Measured and simulation results of rectifier circuit on (A) voltage and (B) power

reaches to 36.22 mW with the bridge rectifier and 37.97 mW with the voltage doubler, respectively. The load resistance at the maximum power is different for the bridge rectifier and voltage doubler, respectively, because each rectifier provides a different source impedance to the resistor load. The harvesting powers are enough high to operate IoT devices but can be increased further placing a matching network before the rectifier circuit.

3.3 | Matching network

The matching network shown in Figure 4C reduces signal reflection between the conducted EMI source and the rectifier circuit. During the matching network design, the inductor L_S over 10 mH is impractical because a high inductance reduces the self-resonance frequency of the inductor below the LF band, at which the matching network is operated. The matching network was designed to have L_S less than 10 mH. In our study, the Coilcraft LPS6235 series was selected for the inductor model due to its low DC resistance and low profile [22]. As before, the matching network was designed using the optimization process provided by ADS.

For the rectifier circuit, its output power was simulated after inserting the matching network between the conducted EMI source and the rectifier. As before, the rectifier terminated the output with a resistor load having increasing resistance. Figure 7 shows the simulation results of the output power of the rectifier. In comparison with Figure 6B, the maximum output power in Figure 7 dramatically increases over 60 mW for the bridge rectifier and 80 mW for the voltage doubler, respectively. This is because the matching network reduces the signal reflection between the conducted EMI source and the rectifier circuit. For the bridge rectifier, its output power is smaller than that of the voltage doubler. This is because L_S in the matching network needs to be higher than 10 mH to reduce the signal reflection completely, but such L_S is impractical due to the low self-resonance frequency as described previously.

Another reason for the lower maximum output power with the bridge rectifier is its structure. As shown in Figure 5A, the bridge rectifier consists of the four Schottky diodes. The input voltage to be rectified is reduced during the forward conduction by the amount equal to the sum of the threshold voltages of the two diodes. The forward voltage drop, however, is reduced by half at the voltage doubler because only one diode reduces the input voltage during the forward conduction. These results are consistent with the fact that the bridge rectifier is not suitable for low power applications [17].

3.4 | Voltage down converter

As shown in Figure 4A, the voltage down converter is used for the final stage of the energy harvester. This down converter provides a regulated output voltage of 3.3 V or 5.0 V. Considering the range of the harvested power from the conducted EMI source, LTC 3632 from

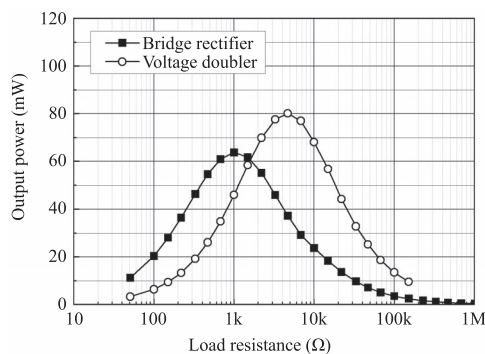


FIGURE 7 Simulation results of rectifier output with matching network

Linear Technology was selected as the down converter model [23].

Figure 8 shows the fabricated energy harvester that consists of the matching network, the voltage doubler, and the voltage down converter, respectively. Each harvester is the same except for the type of the rectifier circuit. The fabricated energy harvester has a compact size of $57 \times 25 \text{ mm}^2$, so it is easy to attach to a lampshade of fluorescent light.

4 | MEASUREMENT RESULTS

As shown in Figure 4A, the power at the output of the rectifier is defined as the harvested power, P_{HAV} , while the power at the output of the voltage down converter as the regulated power, P_{REG} . The fabricated energy harvester shown in Figure 8 was attached to the lampshade of the fluorescent light, and then P_{HAV} and P_{REG} were measured, respectively. As shown in Figure 8, the harvester has the port to measure the rectifier output. P_{HAV} was measured at this port. Figure 9 shows the measured P_{HAVs} and P_{REGs} for the energy harvesters that use the bridge rectifier and the voltage doubler, respectively. As before, P_{HAVs} and P_{REGs} were measured as increasing the load resistance. As shown in Figure 9, the output power of the rectifiers with the down converter, $P_{\text{HAV3.3V}}$ and $P_{\text{HAV5.0V}}$ could be measured at a fewer number of the load resistances than that without the down converter, because the rectifier output voltage is too low when the load resistance is smaller than a specific resistance. Due to such a low voltage, the voltage down converter does not work, so $P_{\text{HAV3.3V}}$ and $P_{\text{HAV5.0V}}$ cannot be measured.

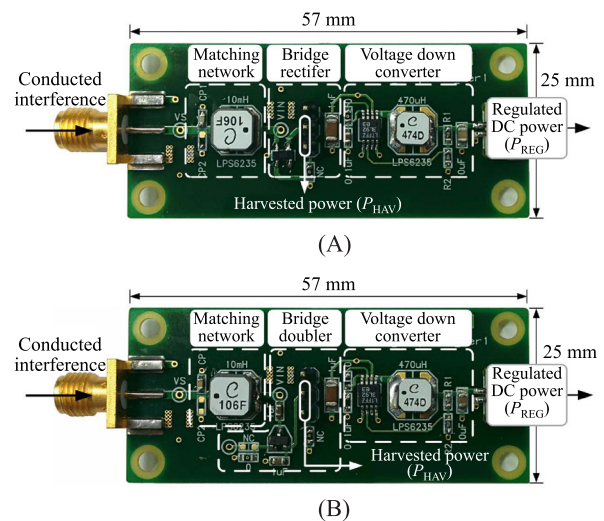


FIGURE 8 Fabricated energy harvester using (A) the bridge rectifier and (B) the voltage doubler

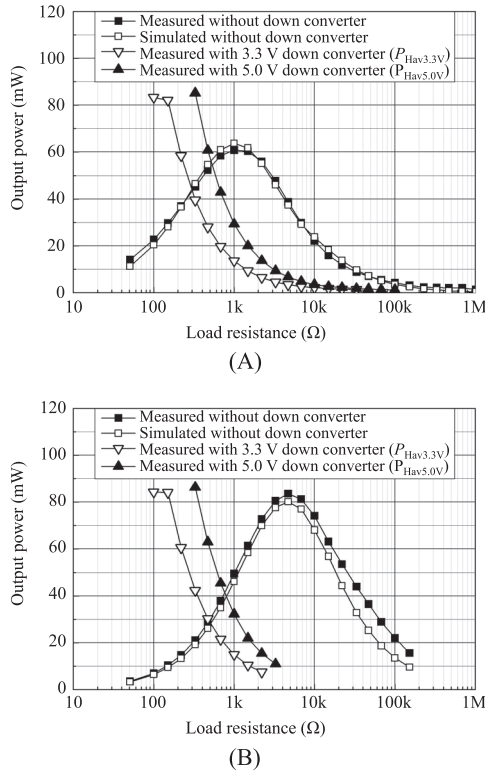


FIGURE 9 Harvested powers when using (A) the bridge rectifier and (B) the voltage doubler

In addition to the measured output power without the down converter, Figure 9 shows the simulated ones in Figure 7 for comparison.

As shown in Figure 9, the measured output powers without down converter are almost the same as the simulated ones. As shown in Figure 9A, the maximum output power with the down converter for the bridge rectifier, $P_{HAV3.3V}$ and $P_{HAV5.0V}$ is higher than that without the down converter. Such a power increase is attributed to the inductance component provided by the voltage down converter. As described in the previous section, the bridge rectifier requires the matching network to have the higher inductance, L_S , over 10 mH in order to reduce the signal reflection further between the conducted EMI source and the rectifier circuit. As shown in Figure 4A, the rectifier circuit is serially connected to the inductor of the matching network. The voltage down converter uses an inductor having a high inductance, and this inductor increase the inductance when the matching network looks into the rectifier circuit. As a result, the voltage down converter provides an additional inductance to the matching network resulting the reduction of the signal reflection; hence, as shown in Figure 9A, the maximum $P_{HAV3.3V}$ and $P_{HAV5.0V}$ are larger than the maximum power without the down converter.

As shown in Figure 9B, the maximum output powers of the voltage with the down converter, $P_{HAV3.3V}$ and $P_{HAV5.0V}$ are slightly higher than that without the down converter. The maximum powers of the two types of rectifiers are almost the same. Figure 10 shows the comparison of the output power of the bridge rectifier and the voltage doubler. In all cases, the maximum output powers for both the bridge rectifier and the voltage doubler are theoretically the same under the condition of a large input voltage where the voltage drop by the threshold voltage is negligible. The maximum difference between each output power compared to the average output of the two rectifiers shows less than 1.2%.

As shown in Figure 7, however, a large difference of 22.8 mW in the output power between the two types of rectifiers with the matching network. This difference is caused by the difference in the input impedance of the two rectifiers and the limited inductance available in the low-frequency band. The input impedance of an n -stage voltage multiplier is reduced by $1/n$ times that of a half-wave rectifier [23]. The voltage doubler has the half capacitive reactance of the bridge rectifier. The bridge rectifier requires a higher inductance to reduce the reflection from the conducted EMI source. Due to the limited inductance of a practical element, the bridge rectifier has less output power. The inductor used in the voltage down converter serves as part of the matching network, hence two rectifiers have the same maximum output power. As a result, if the elements required for the matching network are available, it is assumed that the maximum output power that can be obtainable by the two types of rectifiers should be similar. Considering the limitations of available matching elements, the easy design of the matching network by controlling the number of stages, and the independence from the selection of the voltage step down converter, a voltage multiplier has an advantage as the conducted EMI harvester.

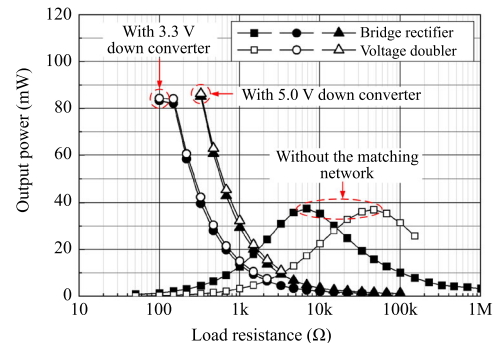


FIGURE 10 Measured output power of the bridge rectifier and the voltage doubler

TABLE 1 Summary of measurement results

Parameters	Unit	Bridge rectifier		Voltage doubler	
Output voltage of energy harvester	V	3.3	5.0	3.3	5.0
Load resistance, R_{Load}^a	Ohm	150	471	150	328
Max. regulated power, P_{REG}^a	mW	70.3	75.8	68.9	75.5
Max. regulated voltage, V_{REG}^a	V	3.27	5.00	3.23	4.99
Max. regulated current, I_{REG}^a	mA	21.5	15.2	21.4	15.1
Conversion efficiency of down converter	%	85.6	89.1	81.9	87.4

^aSee Figure 4A for meaning of symbols.

TABLE 2 Comparison with other studies on fixed-type energy harvesting from fluorescent light

	[13]	[11]	[25]	[26]	[12]	Our
Source type	MF	MF	MF	MF	EF	CE
Source current for MF or power for EF	8.5 A	30 W	10 A	90 W	64 W	64 W
Harvesting (regulated) power (mW)	50	0.6	63.72	7.5	0.8	68.9–75.8

Abbreviations: CE, conducted EMI; EF, electric field of spurious EM waves; MF, magnetic field around current wire.

The proposed conducted EMI energy harvesting has been successfully implemented enough to power various IoT devices. As shown in Figure 1, the adhesive conductive electrode is used to capture the conducted EMI signal and install the harvesting board on the conductive part of the fluorescent light. The regulated output voltage directly drives the IoT devices.

Table 1 summarizes the measurement results of the energy harvester in our study. In addition to the maximum P_{REG} , it presents the voltage, V_{REG} , and the current, I_{REG} , respectively, both of which are defined in Figure 4A. All the measurement results correspond to when the voltage down converter regulates its output voltage to 3.3 V. Table 1 also presents the measurement results when the regulated voltage is 5.0 V. As the regulated voltage increases to 5.0 V, the conversion efficiency of the down converter increases, which is an inherent property of the voltage down converter according to [24].

Table 2 presents the comparison of the measurement results with previous studies. As the current or power of the harvesting source decreases, the harvesting power also decreases. The energy harvester in our study, however, results in the highest power even though the source power is in the medium range. In our study, the energy harvester provides the regulated power over 68.9 mW and current over 15.1 mA, respectively. Such the regulated power and current are enough to operate IoT devices including temperature and humidity sensors, but also Zigbee and MiMax nodes for data communication [2]. As a result, the proposed harvesting technology is practical in that the harvesting performance is enough to

operate IoT devices without combination with other types of harvesting sources such as solar, thermal, and vibration ones.

5 | CONCLUSION

This paper proposes an energy harvesting that harvests from a conducted EMI signal on the surface of a fluorescent light. The source of the conducted EMI signal was modeled from the measurement results, and the source model was used to design the energy harvester including the matching network, the rectifier circuit, and the voltage down converter, respectively. The energy harvester uses two types of the rectifier circuits: the bridge rectifier and the voltage doubler, respectively. The energy harvester produces the regulated power over 68.9 mW and current over 15.1 mA. In comparison with previous studies, the regulated power is highest while the harvesting source has the medium-range power. The proposed harvesting technology is advantageous in that the energy harvesting can be achieved simply by attaching the energy harvester on the surface of a fluorescent light while the regulated power and current produced by the energy harvester are high enough to operate various IoT devices supporting data communication.

ACKNOWLEDGMENTS

This work was supported by Institute of Information and Communications Technology Planning and Evaluation (IITP) grant funded by the Korea government (MSIT)

(2021-0-00103, “Research and development of technologies for utilization of THz frequency band and evaluation of electromagnetic safety”).

CONFLICT OF INTEREST

The authors declare that there are no conflicts of interest.

ORCID

Chang-Hee Hyung  <https://orcid.org/0000-0002-9012-2217>

Jung-Hwan Hwang  <https://orcid.org/0000-0002-6072-0443>

REFERENCES

- O. B. Akan, O. Cetinkaya, C. Koca, and M. Ozger, *Internet of hybrid energy harvesting things*, IEEE Internet Things J. **5** (2018), no. 2, 736–746.
- S. Zeadally, F. K. Shaikh, A. Talpur, and Q. Z. Sheng, *Design architectures for energy harvesting in the Internet of Things, Renew, Sustain. Energy Rev.* **128** (2020), no. 2, 736–746.
- Y. K. Tan and S. K. Panda, *Energy harvesting from hybrid indoor ambient light and thermal energy sources for enhanced performance of wireless sensor nodes*, IEEE Trans. Ind. Electron. **58** (2011), no. 9, 4424–4435.
- H. Lhermet, C. Condemine, M. Plissonnier, R. È. Salot, P. Audebert, and M. Rosset, *Efficient power management circuit: From thermal energy harvesting to above-IC microbattery energy storage*, IEEE J. Solid-State Circuits **43** (2008), no. 1, 246–255.
- N. J. Guilar, R. Amirtharajah, P. J. Hurst, and S. H. Lewis, *An energy-aware multiple-input power supply with charge recovery for energy harvesting applications*, (IEEE International Solid-State Circuits Conference - Digest of Technical Papers, San Francisco, CA, USA), Feb. 2009. <https://doi.org/10.1109/ISSCC.2009.4977426>
- S. Bandyopadhyay and A. P. Chandrakasan, *Platform architecture for solar, thermal, and vibration energy combining with MPPT and single inductor*, IEEE J. Solid-State Circuits **47** (2012), no. 9, 2199–2215.
- A. Nasiri, S. A. Zabalawi, and G. Mandic, *Indoor power harvesting using photovoltaic cells for low-power applications*, IEEE Trans. Ind. Electron. **56** (2009), no. 11, 4502–4509.
- D. Pubill, J. Serra, and C. Verikoukis, *Harvesting artificial light indoors to power perpetually a wireless sensor network node*, (IEEE 23rd International Workshop on Computer Aided Modeling and Design of Communication Links and Network, Barcelona, Spain), Sept. 2018. <https://doi.org/10.1109/CAMAD.2018.8514995>
- K. Geissdoerfer, F. Schmidt, and B. Kusy, *Demo abstract: Bootstrapping batteryless networks using fluorescent light properties*, (ACM/IEEE International Conference on Information Processing in Sensor Networks, Sydney, Australia), Apr. 2020. <https://doi.org/10.1109/IPSIN48710.2020.000-8>
- C. H. Hyung, J. H. Hwang, J. H. Lee, S. W. Kang, and Y. T. Kim, *Energy harvesting from electromagnetic interference induced in the human body*, Electron. Lett. **52** (2016), no. 22, 1881–1883. <https://doi.org/10.1049/el.2016.3049>
- G. Monti, P. Arcuti, F. Congedo, and L. Tarricone, *Power generation by spurious emissions from compact fluorescent lamps*, (44th European Microwave Conference, Ome, Italy), Oct. 2014. <https://doi.org/10.1109/EuMC.2014.6986550>
- O. Cetinkaya and O. B. Akan, *Electric-field energy harvesting from lighting elements for battery-less Internet of Things*, IEEE Access **5** (2017), 7423–7434. <https://doi.org/10.1109/ACCESS.2017.2690968>
- J. Hou, S. Wang, S. Zhang, Q. She, Y. Zhu, and C. Li, *Design and application of a CT-based high-reliability energy harvesting circuit for monitoring sensors in power system*, IEEE Access **7** (2019), 149039–149051. <https://doi.org/10.1109/ACCESS.2019.2946325>
- F. Yang, L. Du, H. Yu, and P. Huang, *Magnetic and electric energy harvesting technologies in power grids: A review*, Sensors **20** (2020), no. 5, 1496.
- F. Giezendanner, J. Biela, J. W. Kolar, and S. Zudrell-Koch, *EMI noise prediction for electronic ballasts*, IEEE Trans. Power Electron. **25** (2010), no. 8, 2133–2141.
- EN 55015, *Limits and methods of measurement of radio disturbance characteristics of electrical lighting and similar equipment*, CENELEC, Brussels, Belgium, 2006.
- L. C. Long, W. E. Sayed, V. Munesswaran, N. Moonen, R. Smolenski, and P. Lezynski, *Assessment of conducted emission for multiple compact fluorescent lamps in various grid topology*, Electronics **10** (2021), no. 18, 2258.
- B. Merabet, F. Costa, H. Takhedmit, C. Vollaire, B. Allard, L. Cirio, and O. Picon, *A 2.45-GHz localized elements rectenna, microwave, antenna*, (3rd IEEE International Symposium on Microwave, Antenna, Propagation and EMC Technologies for Wireless Communications, Beijing, China), Oct. 2009. <https://doi.org/10.1109/MAPE.2009.5355628>
- T. Le, J. Han, A. Von Jouanne, K. Mayaram, and T. S. Fiez, *Piezo-electric power generation interface circuits*, (Proceedings of the IEEE 2003 Custom Integrated Circuits Conference, San Jose, CA, USA), Sept. 2003. <https://doi.org/10.1109/CICC.2003.1249447>
- S. Keyrouz, H. J. Visser, and A. G. Tjihuis, *Multi-band simultaneous radio frequency energy harvesting*, (7th European Conference on Antennas and Propagation, Gothenburg, Sweden), Apr. 2013.
- Avago Technologies, *HSMS-280x*. Available from: <http://www.avagotech.com/docs/AV02-0533EN>
- Coilcraft, *LPS6235*. Available from: <https://www.coilcraft.com/en-us/products/power/shielded-inductors/ferrite-drum/lps/lps6235/>
- S. Keyrouz, H. Pflug, and H. Visser, *Input impedance calculation of a multi-stage rectifier circuit*, (IEEE Wireless Power Transfer Conference, London, UK), June 2019. <https://doi.org/10.1109/WPTC45513.2019.9055683>
- Linear Technology, *LTC3632*. Available from: <http://www.linear.com/product/LTC3632>
- Z. Wu, Y. Wen, and P. Li, *A power supply of self-powered online monitoring systems for power cords*, IEEE Trans. Energy Convers. **28** (2013), no. 4, 921–928.
- J. Moon, J. Donnal, J. Paris, and S. B. Leeb, *VAMPIRE: A magnetically self-powered sensor node capable of wireless transmission*, (Twenty-Eighth Annual IEEE Applied Power Electronics Conference and Exposition, Long Beach, CA, USA), Mar. 2013. <https://doi.org/10.1109/APEC.2013.6520751>

AUTHOR BIOGRAPHIES



Chang-Hee Hyoung received the BS and MS degrees in electronic engineering from Kwangwoon University, Seoul, Republic of Korea, in 1996 and 1998, respectively, and the PhD degree in information and communication engineering from the Korea Advanced Institute of Science and Technology, Daejeon, Republic of Korea, in 2013. Since 1999, he has been with the Electronics and Telecommunications Research Institute (ETRI), Daejeon, Republic of Korea, where he is currently a Principal Engineer with the Radio Environment and Monitoring Research Group. He has been primarily involved in the design and development of analog and RF circuits for wireless network. His research interests include short-range communication system and energy harvesting system from electromagnetic field.



Jung-Hwan Hwang received the BS and MS degrees in electronic engineering from Chungnam National University, Daejeon, Republic of Korea, in 1998 and 2000, respectively, and the PhD degree in information and communication

engineering from the Korea Advanced Institute of Science and Technology, Daejeon, Republic of Korea, in 2016. From 2000 to 2002, he was a Research Engineer with Knowledge-on Inc., Iksan, Republic of Korea, where he focused on the development of microwave circuits. Since 2002, he has been with the Electronics and Telecommunications Research Institute, Daejeon, Republic of Korea, where he is currently a Senior Engineer. He has been primarily involved in the radio channel modeling. His current research interests include electromagnetic compatibility, electromagnetic fields safety, and health effects.

How to cite this article: C.-H. Hyoung and J.-H. Hwang, *Energy harvesting from conducted electromagnetic interference of fluorescent light for Internet of Things application*, ETRI Journal (2022), 1–10. <https://doi.org/10.4218/etrij.2021-0255>